Available online at www.sciencedirect.com
ScienceDirect
Journal of Solid State Chemistry 180 (2007) 461–466
JOURNAL OF SOLID STATE CHEMISTRY
www.elsevier.com/locate/jssc

High-yield synthesis and characterization of monodisperse sub-microsized $CoFe_2O_4$ octahedra

Xian-Ming Liu[a], Shao-Yun Fu[b,*], Lu-Ping Zhu[b]

[a]*Department of Chemistry, Luoyang Normal University, Luoyang 471022, PR China*
[b]*Technical Institute of Physics and Chemistry, Chinese Academy of Sciences, Beijing 100080, PR China*

Received 25 August 2006; received in revised form 28 October 2006; accepted 4 November 2006
Available online 9 November 2006

Abstract

In this study, sub-microsized $CoFe_2O_4$ octahedra with a high yield are synthesized via a simple hydrothermal route under mild conditions. The as-prepared products are characterized by conventional techniques of XRD, SEM, TEM, ED and HR-TEM. The results show that the as-synthesized sample exhibits octahedral morphology with a narrow size distribution. The edge size of $CoFe_2O_4$ octahedra is estimated to be about 0.10–0.14 μm. The growth process is also monitored by time and temperature-dependent observation. It is found that the reaction temperature has no obvious influence on the product morphology but a significant effect on the size of $CoFe_2O_4$ octahedra, while the reaction time determines the final morphology of the product. Moreover, it is displayed that the citrate ions play a key role in the formation of $CoFe_2O_4$ octahedra. Furthermore, the possible growth mechanism of the sub-microsized $CoFe_2O_4$ octahedra is discussed on the basis of a series of experiments. Magnetic measurements show that sub-micro-sized $CoFe_2O_4$ octahedra exhibit obvious ferromagnetic behaviors. The saturation magnetization (M_s), remanent magnetization (M_r), and coercivity (H_c) are determined to be 85.8, 29.2 emu/g and 892 Oe, respectively.
© 2006 Elsevier Inc. All rights reserved.

Keywords: $CoFe_2O_4$; Octahedron; Hydrothermal; Magnetic measurement

1. Introduction

Transition metal oxides constitute one of the most fascinating classes of inorganic solids, as they exhibit a very wide variety of structures, properties, and phenomena. Oxide materials have been employed in many important advanced technology areas due to their many interesting physical properties, including magnetic, ferroelectric, superconducting, ionic and electrical conducting characteristics [1–4]. Among the family of ferrite materials, cobalt ferrite ($CoFe_2O_4$), with a partially inverse spinel structure, is one of the most important and abundant magnetic materials. As a conventional magnetic material with a Curie temperature (T_c) around 793 K, $CoFe_2O_4$ is well known to have large magnetic anisotropy, moderate saturation magnetization, remarkable chemical stability and a mechanical hardness, which makes it a good candidate for the recording media [5].

Some synthetic methods have been developed to prepare $CoFe_2O_4$ ferrites. These synthetic methologies include thermal decomposition [6], reverse micelles [7], coprecipitation [8], micro-emulsion procedures [9–15], precursor techniques [16–20], alkalide reduction [21], sonochemical reactions [22], sol–gel techniques [23–25], host template [26,27], solvo/hydrothermal method [28,29], combustion method [30], and mechanical alloying [31–33] for the fabrication of stoichiometric and chemically pure spinel ferrite powders. The irregularity of particle morphology and the agglomeration of particles still remain the main problems. Among these synthetic methods, the hydrothermal methods have been extensively used to prepare diversiform particles due to the good controllability of particle morphology. In addition, the hydrothermal synthesis requires neither extremely high processing temperature nor sophisticated processing. Very recently, the synthesis of magnetic octahedrons has been recognized as a very

*Corresponding author. Fax: +(86) 108 254 3752.
E-mail address: syfu@cl.cryo.ac.cn (S.-Y. Fu).

0022-4596/$ - see front matter © 2006 Elsevier Inc. All rights reserved.
doi:10.1016/j.jssc.2006.11.003

important issue. Microsized $MnFe_2O_4$ [34] and Fe_3O_4 [35] octahedrons have been synthesized via the hydrothermal method under certain conditions. Nickel ferrite octahedra with broad size distribution have been successfully prepared by a simple hydrothermal route [36]. Zhang et al. reported that micro-sized (4 μm) $CoFe_2O_4$ octahedrons have been synthesized by an EDTA-assisted route under hydrothermal conditions [37]. However, there is no report on the controllable synthesis of $CoFe_2O_4$ particles using citrate ions as directing agent. Citrate is an important biological ligand for metal ions. Citrate salts have been introduced as shape modifier and proved to be efficient to control the shape of some compounds's (ZnO and $CaC_2O_4 \cdot H_2O$) nanostructures [38–40].

Herein, we report a facile hydrothermal method to synthesize single crystalline sub-micro-sized $CoFe_2O_4$ octahedra with a high yield, in which citrate salts have been introduced to control over the precipitate procedure. Moreover, our products show high saturation magnetization and coercivity at 300 K, which may inspirit more convenient access to the exploration of magnetic materials with special morphology.

2. Experimental

All the reagents used in the experiments were in analytical grade (purchased from Beijing Chemical Industrial Co.) and used without further purification. A typical approach employed in this work is given as follows. To prepare ferrite particles, $(NH_4)_2Fe(SO_4)_2 \cdot 6H_2O$ (0.5 g, 1.28 mmol) and $C_6H_5Na_3O_7 \cdot 2H_2O$ (0.86 g, 4.72 mmol) were dissolved in 20 mL of distilled water under constant stirring for 30 min at room temperature, then stoichiometric $CoCl_2 \cdot 6H_2O$ (0.15 g, 0.64 mmol) was added and disolved. The green solution turned into a laurel-green solution gradually. Subsequently, 20 mL of 5 mol/L NaOH solution was slowly dripped without stirring. Greenish precipitate could be observed at that time. The molar ratio of Co (II) to Fe (II) in the above system was 1:2. Afterwards, the mixtures were transferred into a 50 mL Teflon-lined autoclave, maintained at 120 °C for 24 h. The black powders collected from the bottom of the container were washed with distilled water and absolute alcohol in turns, vacuum-dried, and kept for further characterization.

To reveal the crystalline structure of the black powders, XRD analysis was carried out on a Regaku D/max2500 diffractometer at a voltage of 40 kV and a current of 200 mA with Cu-$K\alpha$ radiation ($\lambda = 1.5406$ Å), employing a scanning rate of $0.02^\circ s^{-1}$ in the 2θ ranging from 5° to 80°. Conventional TEM image, high resolution TEM and the electron diffraction (ED) patterns were recorded on JEM-2010 transmission electron microscope with an accelerating voltage of 200 kV. The scanning electron microscopy (SEM) images were obtained using a HITACHI S-4300 microscope. Magnetic measurements were performed on a Quantum Design MPMS-7 superconducting quantum interference device (SQUID) magnetometer. The actual stoichiometric compositions of the obtained powders were determined by a Shimadzu ICPS-75000 inductively coupled plasma atomic emission spectrometer (ICP-AES).

3. Results and discussion

Fig. 1 shows XRD patterns of cobalt ferrite powders prepared by the hydrothermal route at 120 °C under different alkaline concentration. The diffraction patterns and relative intensities of all diffraction peaks matched well those of standard data (JCPDS card No. 22-1086) for $CoFe_2O_4$. The strong peaks appeared at around 18.5°, 30.2°, 35.6°, 37.2°, 43.0°, 53.4°, 57.1°, and 62.5° that are well indexed to the crystal plane of spinel ferrite (111), (220), (311), (222), (400), (422), (511), and (440), respectively. The peak intensity of $CoFe_2O_4$ increased with the increase of the NaOH concentration, which indicated that the NaOH concentration played a role in the formation of spinel crystal structure and morphology. All the ferrites showed a single-phase spinel ferrite with no impurities in the XRD patterns. In addition, the elemental analyses of these particles using ICP-AES showed that the molar ratios of Co^{2+}/Fe^{3+} are near to 1:2.

The SEM images in Fig. 2 show the morphology of $CoFe_2O_4$ powders prepared by a simple hydrothermal method at different alkaline concentrations. It can be seen from Fig. 2 that the NaOH concentration plays an important role in the morphology of the final products. The ferrites exhibit quasi-hexahedral morphology at low concentration, while the hydrothermal product is octahedral at high concentration. In addition, the yield of $CoFe_2O_4$ octahedra is very high under this hydrothermal condition. The facets of the octahedra are apparently distinguishable, as is further revealed at high magnification in Fig. 2(c). The size of the $CoFe_2O_4$ octahedra ranges from 100 to 200 nm and their edge size is about 100–140 nm.

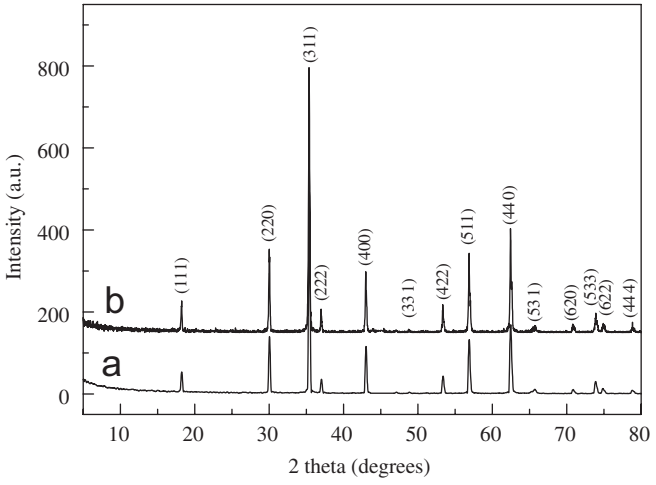

Fig. 1. PXRD patterns of $CoFe_2O_4$ powders prepared by the hydrothermal route at 120 °C under different alkaline concentration: (a) 1.25 M; (b) 2.5 M.

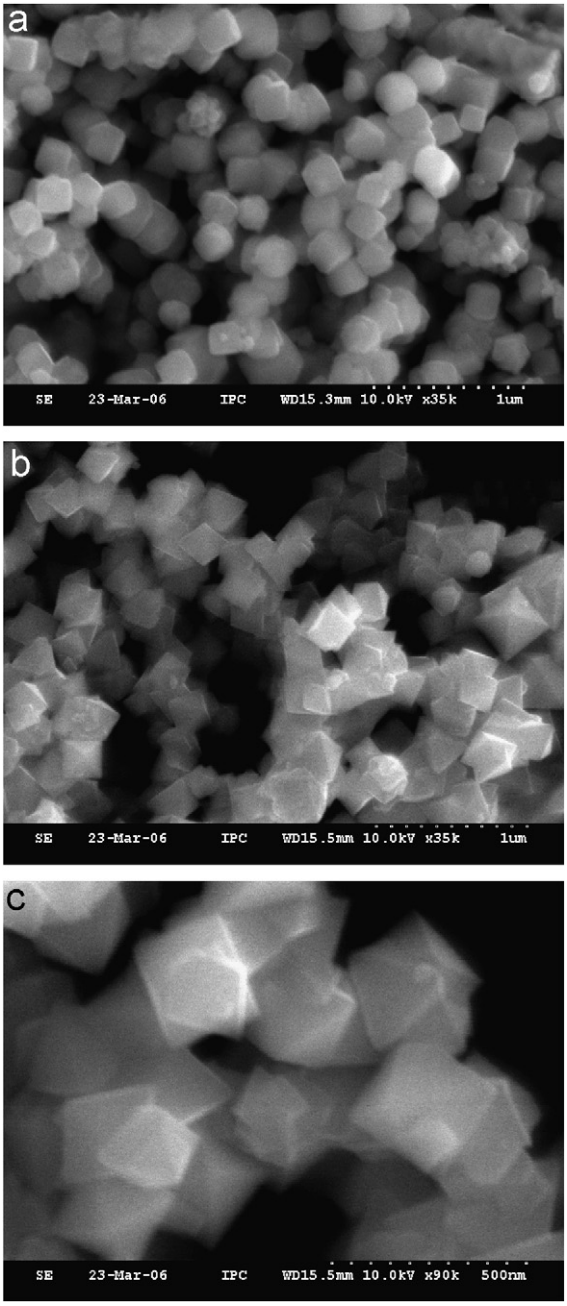

Fig. 2. (a) SEM images of the samples synthesized by hydrothermal method at 120 °C for 24 h under 1.25 M NaOH concentration; (b) 2.5 M NaOH concentration at low magnification; (c) 2.5 M NaOH concentration at high magnification.

Further observation on the facet structure of the hydrothermal product at 2.5 M NaOH concentration was conducted by conventional TEM, HRTEM, and ED. Fig. 3(a) shows the direct projection morphology of octahedrons with narrow size distribution, from which the high geometric symmetry of the octahedrons can be obtained. The edge size of $CoFe_2O_4$ octahedra is estimated to be 100–140 nm. ED pattern (Fig. 3(b)) corresponding to bright field images, shows that these particles consist of Co ferrite crystals with an inverse spinel structure, consistent with the XRD result. ED patterns on different individual crystal were essentially the same, indicating that $CoFe_2O_4$ octahedrons are single-crystalline in structure.

High-resolution TEM images provided further insight into the structure of these materials. HRTEM image (Fig. 3(c)) shows that the particles were structurally uniform with an inter-planar spacing about 4.85 Å, as indicated clearly by atomic lattice fringers, which corresponds to the (111) lattice plane of $CoFe_2O_4$ crystals (4.847 Å). A structure model of the octahedron enclosed by {111} planes is presented in Fig. 3(d). The shape of crystals is mostly determined by the relative growth rate between different directions during their formation. It is known that particles usually have specific shape because a single-crystal particle has to be enclosed by crystallographic facets that have lower energy. Therefore, it is believed that the formation of $CoFe_2O_4$ octahedrons during the hydrothermal process proceeds in a way with much faster growth rate along $\langle 001 \rangle$ than along {111} due to the lowest energy of the {111} surfaces.

The growth process was monitored by temperature-dependent observations. Fig. 4(a–d) shows SEM images of the products that were obtained after hydrothermal treatment at different temperatures for 24 h. When the hydrothermal temperature is 100 °C, the as-prepared product is not black and its morphology exhibits irregular shape as shown in Fig. 4(a). The morphology of $CoFe_2O_4$ becomes octahedron-like with the increase of hydrothermal temperature. In other words, the reaction temperature higher than 120 °C has no obvious influence on the morphology of the products. But the size of $CoFe_2O_4$ octahedrons increases with the increase of hydrothermal temperature. At 180 °C, the size of $CoFe_2O_4$ octahedrons is in the range of 200–400 nm.

To understand the formation mechanism of the octahedral structure, time-dependent experiments were carried out by quenching the Teflon-lined autoclave using cold water at different reaction stages. When the hydrothermal time is lower than 12 h, the as-prepared products consist of precipitation of hydroxide caused by incomplete reaction. With the increase of hydrothermal time, the products exhibit unitary component and uniform morphology. A series of SEM images in Fig. 5(a–c) show the morphology at different reaction stages corresponding to the reaction time of 12, 16, and 20 h, respectively. It was shown that aggregated $CoFe_2O_4$ nanocrystals with nearly spheridal morphology (Fig. 5(a)) emerged as the initial product after the reaction proceeded for 12 h. When prolonging the reaction time to 16 h, polyhedral particles grew out on these aggregated particles (Fig. 5(b)). This process of crystal growth and morphology evolution can be described in terms of Ostwald ripening, which involves the growth of large particles at the expense of the smaller ones driven by the tendency of the solid phase in the systems to adjust themselves to achieve a minimum total surface free energy. When increasing the reaction time to 20 h, most of the products were ready to evolve into octahedral structures (Fig. 5(c)). With longer reaction times, smoother crystal

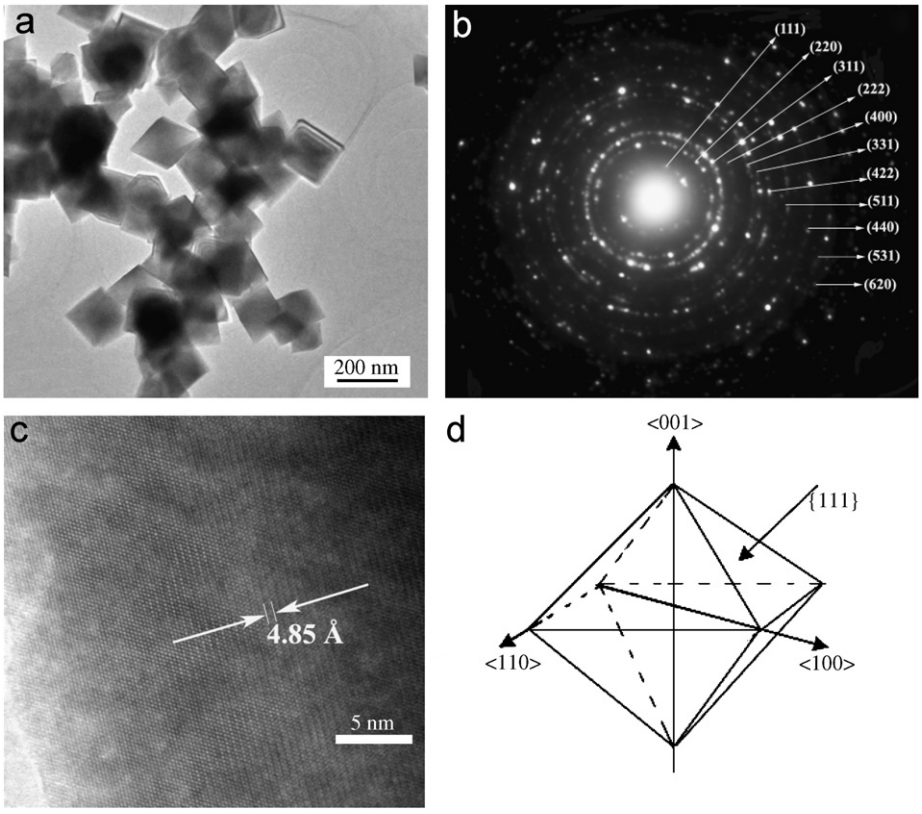

Fig. 3. TEM image (a), ED pattern (b), HR-TEM image (c) and structure model (d) of sub-micro-sized $CoFe_2O_4$ octahedrons.

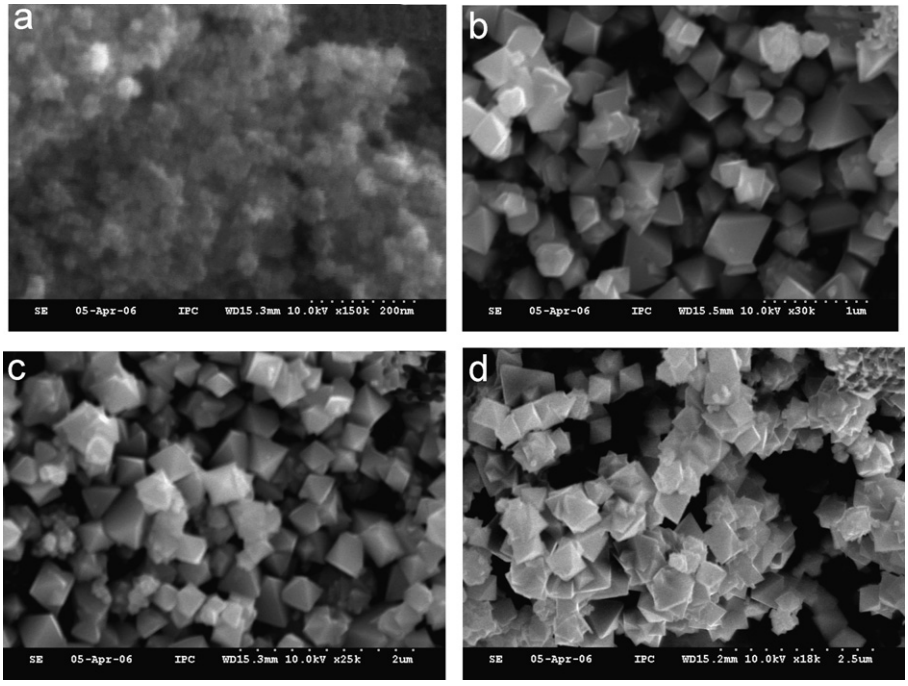

Fig. 4. SEM images of the samples synthesized by hydrothermal method at different temperatures in 2.5 M NaOH solution: (a) 100; (b) 140; (c) 160; (d) 180 °C.

facets can be attained for $CoFe_2O_4$ octahedra due to continuous surface flattening. The formation process for $CoFe_2O_4$ octahedra is shown in Fig. 5(d).

Regarding the growth process, it is believed that citrate plays a crucial role in the formation of $CoFe_2O_4$ octahedra. For the controlled experiment in the absence of citrate by

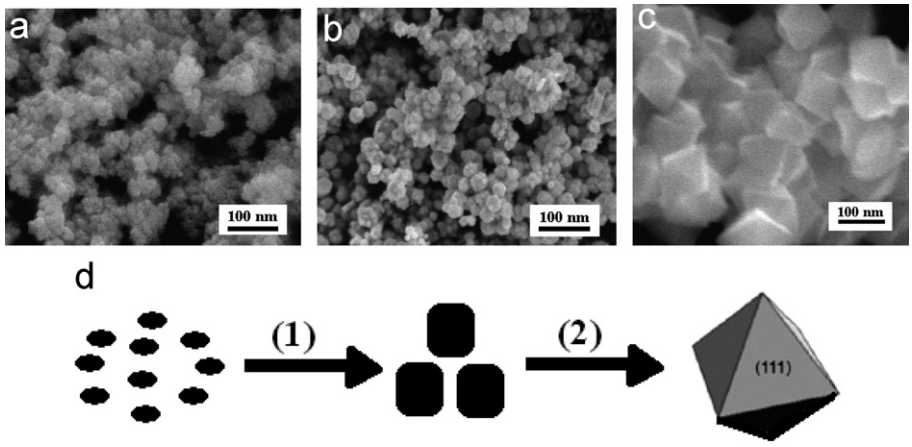

Fig. 5. SEM images of the products obtained from different reaction time: (a) 12; (b)16; (c) 20 h; (d) schematic diagram of the formation process for sub-micro-sized $CoFe_2O_4$ octahedrons.

keeping all other reaction conditions the same, the product is not black $CoFe_2O_4$, but brown mixtures. Citrate anions with three carboxylic groups have a certain binding affinity to metal atoms and can be absorbed on the $CoFe_2O_4$ nanoparticle surfaces when the nanoparticles start growing. The stereochemical characteristics of citrate molecules lead to multiple binding sites for the three carboxylic acid groups when interacting with crystal surfaces. Furthermore, hydrogen bond formation between the citrate hydroxyl group and the oxygen atom within the crystal plane plays a pivotal role in stabilizing the attachment during growth [38–40]. The interaction between surface-adsorbed citrate would be instead of that between the particles themselves, which may yield ordered crystal growth and lead to formation of these ocahedra. In our synthesis, we found that the combinations of metal ions with OH^- could be postponed in citrate solution. The relatively slow reaction is favorable for separating the growth step from the nucleation step and responsible for the narrow size distribution. Under hydrothermal conditions, $CoFe_2O_4$ crystal should grow preferentially and the dehydration steps are repeated in the following procedures. Further studies are necessary to understand the exact growth mechanism because it may open up new opportunities to fabricate more complex nanostructured materials.

The magnetic properties of $CoFe_2O_4$ octahedrons have been studied by measuring the magnetization as a function of temperature in applied field of 50 Oe. Typical M–T curve is shown in Fig. 6(a), from which one can see that the magnetization in the temperature range of 2–350 K increases sharply with the decrease of the temperature. The ferrite octahedra show an obvious ferromagnetic behavior. Hysteresis loop of the sample at 300 K is presented in Fig. 6(b). At 300 K, the $CoFe_2O_4$ octahedrons exhibit hysteresis loop typical of magnetic behaviors, indicating that the presence of an ordered magnetic structure can exist in the spinel system. The magnetization of the sample is much higher and tends to be saturated at a high field. The saturation magnetization of octahedral

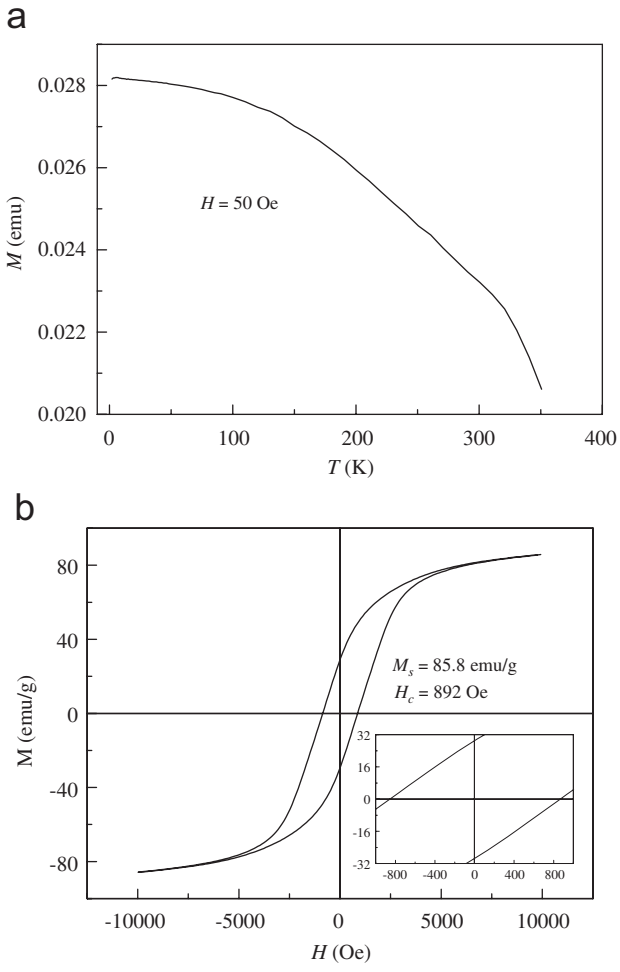

Fig. 6. Magnetic properties of sub-micro-sized $CoFe_2O_4$ octahedrons prepared by hydrothermal method at 120 °C in 2.5 M alkaline solution. (a) Magnetization versus temperature curve; (b) hysteresis loop curve at 300 K; below-right inset of Fig. 6b shows hysteresis loop of low field.

$CoFe_2O_4$ exhibits 85.8 emu/g at 10 kOe, which is close to the saturation magnetization of bulk cobalt ferrite [41]. It can be clearly seen from below-right inset of Fig. 6(b) that

the octahedral $CoFe_2O_4$ has a remanent magnetization of 29.2 emu/g and a coercive field of 892 Oe, respectively. The coercivity of sub-micro-sized $CoFe_2O_4$ octahedra is near to that of the bulk ferrite (980 Oe), but much larger than the reported data (545 Oe) [37]. It is well known that the size has significant influence on their magnetic properties. For relatively larger particles, magnetic domains are formed to reduce the static magnetic energy. The deviation is likely due to the sample structure and small amount of octahedra existing in the sample.

4. Conclusions

In summary, Co ferrite octahedrons with uniform morphology have been synthesized through a facile hydrothermal method using citrate molecules as growth controller, as well as agglomeration inhibitor. For the synthesis of Co ferrite octahedrons, hydrothermal treatment is applied, which is a suitable synthetic route for material preparation under mild conditions (low temperature). This method allows the shape control and high yield, namely two very important aspects for practical applications. The morphology of octahedron enclosed by {111} planes implies much faster growth rate along $\langle 001 \rangle$ than {111} directions during the formation of ferrite phase. In addition, the suitable reaction conditions are very important for the growth of Co ferrite octahedra. Furthermore, our products show high saturation magnetization and coercivity at 300 K, which may inspirit more convenient access to the exploration of magnetic materials with uniform morphology.

Acknowledgements

We gratefully acknowledge the financial support from the Overseas Outstanding Scholar Foundation of the Chinese Academy of Sciences (Grant Nos.: 2005-1-3 and 2005-2-1) and the National Natural Science Foundation of China (Grant No. 50573090).

References

[1] J.J. Li, W. Xu, H.M. Yuan, J.S. Chen, Solid State Commun. 131 (2004) 519.
[2] D.C. Jiles, Acta Mater. 51 (2003) 5907.
[3] Y. Torii, T. Suziki, K. Kato, Y. Uwamino, B.H. Choi, M.J. Lee, J. Mater. Sci. 31 (1996) 2603.
[4] D.J. Singh, M. Gupta, R. Gupta, Phys. Rev. B., 65.064432.
[5] L. Piraux, J.M. George, J.F. Despres, C. Leroy, E. Ferain, R. Legras, K. Ounadjela, A. Fert, Appl. Phys. Lett. 65 (1994) 2484.
[6] T. Hyeon, Y. Chung, J. Park, S.S. Lee, Y.-W. Kim, B.H. Park, J. Phys. Chem. B 106 (2002) 6831.
[7] C.T. Seip, E.E. Carpenter, C.J. O'Connor, J. Vijay, S. Li, IEEE Trans. Magn. 34 (1998) 1111.
[8] Y.I. Kim, D. Kim, C.S. Lee, Physica B 337 (2003) 42.
[9] N. Moumen, M.P. Pileni, Chem. Mater. 8 (1996) 1128.
[10] N. Moumen, M.P. Pileni, J. Phys. Chem. B 100 (1996) 1867.
[11] V. Pillai, D.O. Shah, J. Magn. Magn. Mater. 163 (1996) 243.
[12] J.A. Lopez Perez, M.A. Lopez Quintela, J. Mira, J. Rivas, S.W. Charles, J. Phys. Chem. B 101 (1997) 8045.
[13] N. Feltin, M.P. Pileni, Langmuir 13 (1996) 3927.
[14] N. Moumen, P. Veillet, M.P. Pileni, J. Magn. Magn. Mater. 149 (1995) 67.
[15] C. Liu, B. Zou, A.J. Rondinone, Z.J. Zhang, J. Am. Chem. Soc. 122 (2000) 6263.
[16] B.S. Randhawa, J. Mater. Chem. 10 (2000) 2847.
[17] S. Prasad, N.S. Gajbhiye, J. Alloy. Comp. 265 (1998) 87.
[18] F. Li, J.J. Liu, D.G. Evans, X. Duan, Chem. Mater. 16 (2004) 1597.
[19] X.M. Liu, S.Y. Fu, C.J. Huang, Mater. Sci. Eng. B 121 (2005) 255.
[20] X.M. Liu, S.Y. Fu, H.M. Xiao, Pyhsica B 370 (2005) 14.
[21] K.E. Mooney, J.A. Nelson, M.J. Wagner, Chem. Mater. 16 (2004) 3155.
[22] K.V.P.M. Shafi, A. Gedanken, R. Prozorov, J. Balogh, Chem. Mater. 10 (1998) 3445.
[23] T. Sugimoto, Y. Shimotsuma, H. Itoh, Powder Technol. 96 (1998) 85.
[24] C.S. Kim, Y.S. Yi, K.T. Park, N. Hae, J.G. Lee, J. Appl. Phys. 85 (1999) 5223.
[25] A. Hutlova, D. Niznansky, J.L. Rehspringer, C. Estournès, M. Kurmoo, Adv. Mater. 15 (2003) 1622.
[26] N.S. Kommareddi, M. Tata, V.T. John, G.L. McPherson, M.F. Herman, Y.S. Lee, C.J. O'Connor, J.A. Akkara, D.L. Kaplan, Chem. Mater. 8 (1996) 801.
[27] C. Pham-Huu, N. Keller, C. Estournès, G. Ehret, J.M. Grenèche, M.J. Ledoux, Phys. Chem. Chem. Phys. 5 (2003) 3716.
[28] H. Deng, X. Li, Q. Peng, X. Wang, J. Chen, Y. Li, Angew. Chem. Int. Ed. 44 (2005) 2782.
[29] L.J. Cote, A.S. Teja, A.P. Wilkinson, Z.J. Zhang, Fluid Phase Equ. 210 (2003) 307.
[30] C.H. Yan, Z.G. Xu, F.X. Cheng, Z.M. Wang, L.D. Sun, C.S. Liao, J.T. Jia, Solid State Commun. 111 (1999) 287.
[31] Y. Shi, J. Ding, X. Liu, J. Wang, J. Magn. Magn. Mater. 205 (1999) 249.
[32] Y. Shi, J. Ding, H. Yin, J. Alloys Compds. 308 (2000) 290.
[33] E. Manova, B. Kunev, D. Paneva, I. Mitov, L. Petrov, C. Estournès, C. D'Orléans, J.L. Rehspringer, M. Kurmoo, Chem. Mater. 16 (2004) 5689.
[34] D. Zhang, X. Zhang, X. Ni, J. Song, H. Zheng, Chem. Phys. Lett. 426 (2006) 120.
[35] X.M. Liu, S.Y. Fu, H.M. Xiao, Mater. Lett. 60 (2006) 2979.
[36] Y. Cheng, Y. Zheng, Y. Wang, F. Bao, Y. Qin, J. Solid State Chem. 178 (2005) 2394.
[37] D.E. Zhang, X.J. Zhang, X.M. Ni, J.M. Song, H.G. Zheng, J. Magn. Magn. Mater. 305 (2006) 68.
[38] Z.R. Tian, J.A. Voigt, J. Liu, B. Mckenzie, M.J. Mcdermott, M.A. Rodriguez, H. Konishi, H.F. Xu, Nat. Mater. 2 (2003) 821.
[39] J. Liang, J. Liu, Q. Xie, S. Bai, W. Yu, Y. Qian, J. Phys. Chem. B 109 (2005) 9463.
[40] S.R. Qiu, A. Wierzbicki, E.A. Salter, S. Zepeda, C.A. Orme, J.R. Hoyer, G.H. Nancollas, A.M. Cody, J.J. De Yoreo, J. Am. Chem. Soc. 127 (2005) 9036.
[41] S.T. Okuno, S. Hashimoto, K. Inomata, J. Appl. Phys. 71 (1992) 5926.